Status of the heavy ion beam probe system in the Large Helical Device[a)]

M. Nishiura,[b)] T. Ido, A. Shimizu, H. Nakano, T. Kato, S. Kato, and Y. Hamada
(LHD Experimental Group)
National Institute for Fusion Science (NIFS), 322-6 Oroshi, Toki, Gifu 509-5292, Japan

V. P. Shevelko
P.N. Lebedev Physical Institute, Leninskii Prospect 53, 119991 Moscow, Russia

R. K. Janev
Macedonian Academy of Sciences and Arts, P.O. Box 428, 1000 Skopje, Macedonia

M. Wada
Departments of Electronics, Doshisha University, Kyotanabe, Kyoto 610-0321, Japan

(Presented 29 August 2007; received 27 August 2007; accepted 31 October 2007; published online 20 February 2008)

A heavy ion beam probe (HIBP) system has been installed into the Large Helical Device (LHD) to measure the spatial profile of the plasma potential and density fluctuations. The optimization of the HIBP system, especially the beam injector, is described. The negative ion beam is required for the MeV beam production in a tandem accelerator. A sputter-type heavy negative ion source has been developed as an intense Au^- beam source to produce Au^+ beams with energy in the MeV range. The extraction electrodes and the Einzel lens system of the ion source have been designed taking into account the beam optics, and installed into the real machine. Throughout the plasma diagnostics on LHD experiments, the consumptions of vaporized caesium and gold target are being characterized for practical operations. In addition, the experimental charge fractions are compared with the theoretical fractions for understanding the charge-changing behavior of Au^- ions and optimizing the fraction of Au^+ ions at the exit of the tandem accelerator of the HIBP system. © *2008 American Institute of Physics.* [DOI: 10.1063/1.2819323]

I. INTRODUCTION

In thermonuclear fusion plasma, the radial electric field and density fluctuations are considered to be the major factors that influence the plasma confinement. A heavy ion beam probe (HIBP) system is one of diagnostic tools for detecting the local potential and density fluctuations simultaneously. Therefore, the HIBP system plays a key role for studying the improvement of plasma confinement. We have installed the HIBP system in the Large Helical Device (LHD), which requires MeV energy beams, because the charged particles must reach in a plasma core with a magnetic field of ~3 T for plasma confinement. The negative ions are required for the beam acceleration of ~6 MeV Au^+ in a tandem accelerator with terminal voltage of ~3 MV. The HIBP system has detected the signal of energy analyzed beams successfully since 2004.[1] In the recent experiments, we have detected the interesting behavior with intermittent plasma potential oscillations. With the extension of LHD plasma operations, a wider observable range of plasma parameters is also required for diagnostics. Under the high electron density ($\sim 10^{20}$ m^{-3}) and the high temperature (~10 keV) plasma operations, the injected (primary) beam current of Au^+ should overcome the attenuation due to electron loss and electron capture processes in collisions with plasma edge neutral and core plasma electrons and ions. In the present setup, the secondary beam of Au^{2+} ions could be detected experimentally at electron densities of $\sim 2 \times 10^{19}$ m^{-3}. From the design of HIBP system, the required primary beam current is considered to be more than 10 μA.

In the test stand, we obtained the Au^- beam current of ~65 μA at the beam energy of 14 keV by the new sputter-type negative ion source.[2] The negative ion source is then moved and operated at the real machine. The status and the remaining issues on the ion source and the charge-changing reactions in the gas targets are reported and discussed in the present paper.

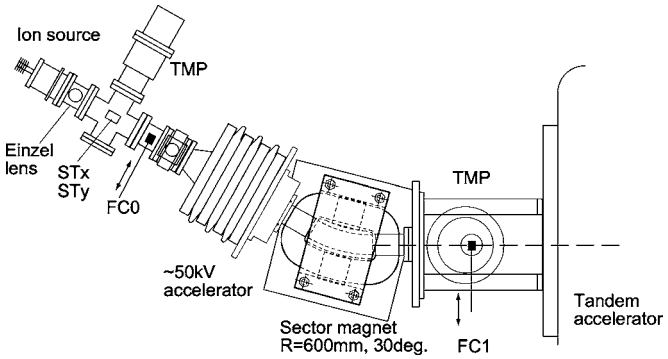

FIG. 1. Schematics of the upstream beam line of the LHD-HIBP system. STx and STy: horizontal and vertical deflector plates. FC0 and FC1: Faraday cups.

[a)] Contributed paper, published as part of the Proceedings of the 12th International Conference on Ion Sources, Jeju, Korea, August 2007.
[b)] Electronic mail: nishiura@nifs.ac.jp.

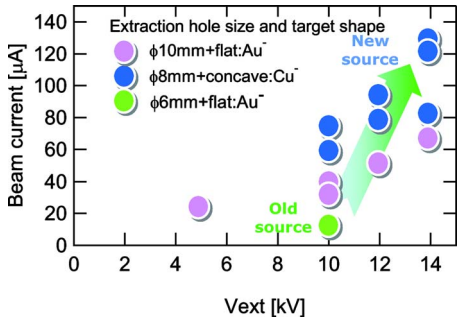

FIG. 2. (Color online) Au^- and Cu^- beam currents for old and new sputter-type negative ion sources as a function of extraction voltage. The data point of $\phi 6$ mm+flat Au^- is measured by the old source for the comparison.

II. GOLD NEGATIVE ION SOURCE

The scheme of the HIBP system on LHD is described in Ref. 1. The beam injection side mainly consists of a sputter-type gold negative ion source, tandem accelerator, beam transport lines, and an octupole electrostatic sweeper. Figure 1 shows the upstream of the beam injection side. Another octupole electrostatic sweeper and the energy analyzer with an array of micro-channel plates are equipped for the beam detection side. These components have been developed continuously.

The Au^- beam current of the plasma-sputter-type negative ion source is characterized as a function of the extraction voltage at the test stand, shown in Fig. 2. The beam current is measured by a Faraday cup located approximately 50 cm downstream from the extraction electrode. The concave shape of Cu target and the flat shape of Au target are also utilized. The Au^- beam current increases with the higher extraction voltage up to 14 kV.

When the plasma-sputter-type negative ion source was moved to the real machine, it has been partly improved. The target holder, the heat shield inside the ion source, the extraction hole, and the Einzel lens are newly designed and replaced to new components, as shown in Fig. 3. These components contribute to the stable beam output and low cesium consumption.

Through the sector magnet, the mass separated beams are detected by the Faraday cup (FC1). The unexpected beam components are negligibly small (only 0.1% for unknown species and 2% for Au_2^-), compared to the Au^- beam.

To estimate the ion source operation hours and its maintenance schedule, the consumptions of sputtering target and cesium are summarized in Table I. The gold target reduces

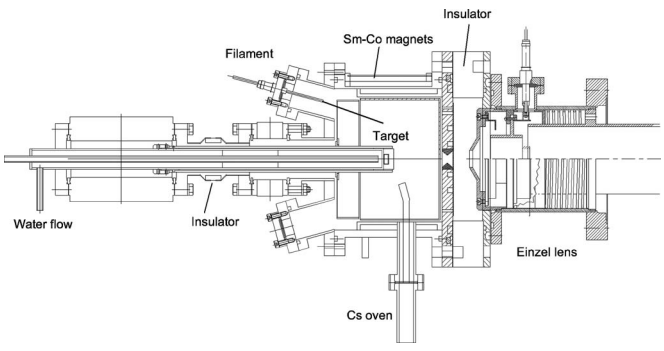

FIG. 3. Plasma-sputter-type negative ion source, extractor, and Einzel lens.

TABLE I. Consumptions of gold target and cesium (estimated twice).

Au target	t 1 mm/132 h
Cs oven	39 mg/h
	44 mg/h
Maximum beam current per day to the tandem	10–17 μA

1 mm thickness during 132 h operation. The cesium consumption in-between cleaning of the ion source is 44 and 39 mg/h, respectively. The confinement of the cesium vapor in the ion source can be improved, because we still found the cesium leakage from the small gaps of the heat shield, and the cesium is deposited at the cold portions of the ion source wall.

III. DESIGN OF EXTRACTOR AND EINZEL LENS

The gold negative ion source described above has been installed into the HIBP system. The extractor and Einzel lens system have been designed by the PBGUNS commercial computer code[3] to obtain well focused beams at the entrance aperture of the 50 kV accelerator. The beam size must be kept within 24 mm in the vertical direction of the duct size, which is limited by the distance between magnetic poles of the existing sector magnet. After the Au^- beam passing through the sector magnet, the diaphragm plate of $\phi 10$ mm is located in front of FC1 in order to inject the good quality beam into the tandem accelerator.

The Au^- beam current is measured at the entrance and the exit of the sector magnet to know the present situation of beam transport and to improve the actual injected beam current into the tandem accelerator. The pair of the voltage of vertical and horizontal beam steering electrodes is located at the downstream of the Einzel lens and is adjusted to positioning the center of the beam. The beam profile is measured by FC0 with the slit of 1 mm in height and 15 mm in width, located at the entrance of the 50 kV accelerator. The measured beam profile, shown in Fig. 4, is integrated over the vertical direction to obtain the total beam current. The Au^- beam current at the energy of 13.9 keV was more than 46 μA by FC0 with the optimum Einzel lens voltage of 13.6 kV. The measured beam diameter at the full width at half maximum is 16.1 mm, which agrees closely with the designed diameter computed by PBGUNS. The measured Au^- beam current was 7 μA by FC1, even though the beam current of 46 μA reaches the same order as that at the test stand. If the diaphragm of $\phi 10$ mm in front of FC1 causes the beam loss, the estimated beam current would be roughly 14 μA. The estimated value is still higher than the measured one at FC1. Therefore the beam is lost partly at the sector magnet, and mainly at the diaphragm of $\phi 10$ mm. The focusing lens system in front of the 50 kV accelerator and the diaphragm of $\phi 10$ mm would be the candidate choices to increase the injected beam current.

IV. FRACTIONS OF HIGHLY CHARGED IONS FROM Au^-

For the optimum operation and further development of the HIBP system, the conversion efficiency from Au^- to Au^+

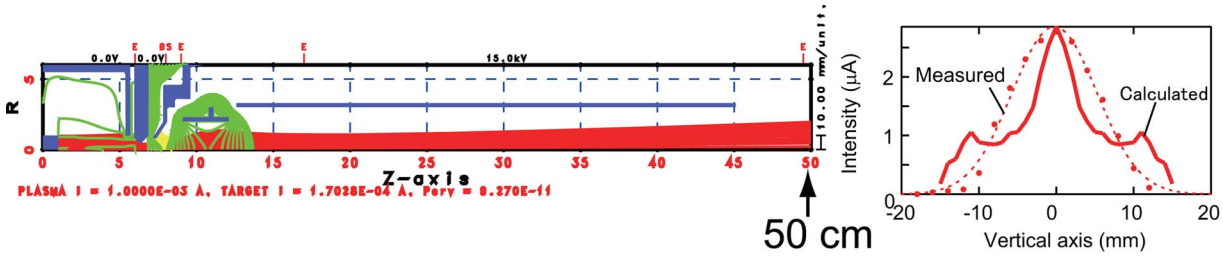

FIG. 4. (Color online) Beam trajectories of plasma-sputter-type negative ion source calculated by PBGUNS. From the left, the Au target inside the ion source cylinder, the extraction electrode, and the Einzel lens are drawn with the Au^- beam at the energy of 13.9 keV. The right figure shows the beam profiles calculated and measured at 50 cm downstream. The relative value of calculated beam profile is plotted.

is assessed experimentally and theoretically. At the projectile beam energy of 3 MeV, the resulting ions are separated by the electrostatic plates at the exit of the tandem accelerator and are measured by the Faraday cup (FC2). The observed fractions are defined as the measured beam current divided by both the charge and the projectile Au^- beam current. Experiments on charge-changing reactions in argon gases are commonly performed at the background gas pressure from 2×10^{-5} to 1.2×10^{-4} Pa. Then the gas pressure inside the gas cell is calibrated relatively using the gas pressure measured by the vacuum gauge at the exit of the tandem accelerator.

The fractions $F(i)$ are calculated numerically solving a set of six differential equations for Au^i component system, where i denotes the ion charge from −1 to +4. The initial value problem is treated for these equations using the Runge-Kutta-Verner fifth-order and sixth-order methods. These sets of equations are integrated over the target thickness nl in cm^{-2} under the initial conditions of $F(-1)=1$, and $F(i)=0$ with $i\geqslant0$.

To solve the above differential equations, we must know the cross sections of elastic scatterings, electron loss, and capture cross sections for all six components. Elastic cross sections are estimated by Biersack and Zeigler's method.[4]

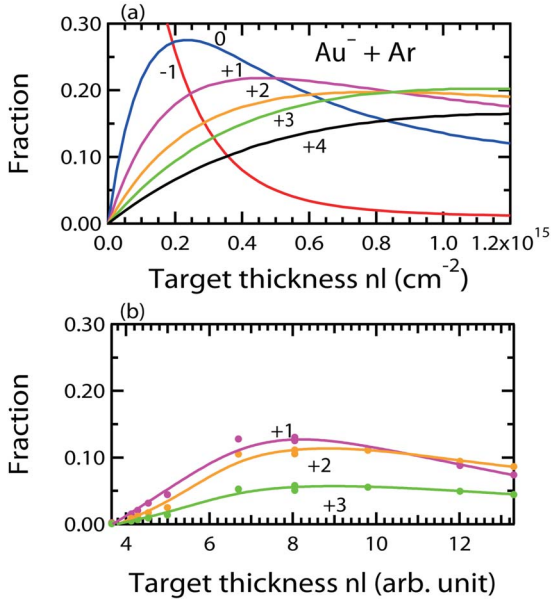

FIG. 5. (Color online) (a) Calculated fractions of Au in Ar gas and (b) measured fractions. Projectile Au^- beam has the energy of 3 MeV.

The cross sections of electron loss processes are calculated by the Firsov model.[5] The cross sections of electron capture processes are calculated using the CAPTURE code,[6] which employs the modified Brinkman-Kramers approximation. The preliminary results of calculated and measured fractions are shown in Figs. 5(a) and 5(b) as a function of target thickness, respectively. By adding the electron capture processes, the calculated fractions are different from those given in the previous report.[7] The results of both calculations and measurements exhibit a similar tendency, but there is a discrepancy in the calculated fraction of Au^{3+}, which exceeds the other positive ion fractions at the high target thickness in the region above 0.8×10^{15} cm^{-2}. This is because the Firsov model describes well the electron loss cross section only for ions having a charge less than + (3–4). The set of differential equations for the ion fractions should include the contribution of charge states up to about $q=+10$ in order to obtain good results for the fraction $F(+3,4)$. In the future work we shall perform charge fraction calculations by using a more sophisticated model for the electron loss processes. In the present calculation, we found that the electron capture processes influence significantly the charge fractions for the target thicknesses above 0.8×10^{15} cm^{-2}. From the experimental aspect, the present experiments still have a margin of enhancement for the Au^+ fraction. According to our prediction, we could enhance the fraction transmitted from 0.13 to 0.22 by controlling the projectile beam optics.

ACKNOWLEDGMENTS

We would like to thank Dr. A. Takagi of KEK, Dr. A. Taniike of Kobe University for their advices, and Dr. H. Tawara of MPI Heidelberg for valuable discussions. This work is supported in part by JSPS Grant No. 18740357, NIFS06KCBR001, and NIFS ULBB505.

[1] T. Ido, A. Shimizu, M. Nishiura, A. Nishizawa, S. Katoh, T. P. Crowley, K. Tsukada, M. Yokota, H. Ogawa, T. Inoue, Y. Hamada, and the LHD Experimental Group, Rev. Sci. Instrum. **77**, 10F523 (2006).
[2] M. Nishiura, T. Ido, A. Shimizu, S. Kato, K. Tsukada, A. Nishizawa, Y. Hamada, Y. Matsumoto, A. Mendenilla, and M. Wada, Rev. Sci. Instrum. **77**, 03A537 (2006).
[3] PBGUNS, Thunderbird Simulations, http://www.thunderbirdsimulations.com
[4] J. P. Biersack and J. F. Ziegler, Nucl. Instrum. Methods Phys. Res. **194**, 93 (1982).
[5] O. B. Firsov, Sov. Phys. JETP **36**, 1076 (1959).
[6] V. P. Shevelko, O. Rosmej, H. Tawara, and I. Yu. Tolstikhina, J. Phys. B **37**, 201 (2004).
[7] A. Taniike, NIFS Report, No. NIFS-352, (1995).